Effects of Stellar Flux on Tidally Locked Terrestrial Planets: Degree-1 Mantle Convection and Local Magma Ponds

The Astrophysical Journal, 735:72 (8pp), 2011 July 10 doi:10.1088/0004-637X/735/2/72

EFFECTS OF STELLAR FLUX ON TIDALLY LOCKED TERRESTRIAL PLANETS: DEGREE-1 MANTLE CONVECTION AND LOCAL MAGMA PONDS

S. E. Gelman[1,2], L. T. Elkins-Tanton[2], and S. Seager[2,3]
[1] Department of Earth and Space Sciences, University of Washington, Box 351310, Seattle, WA 98195, USA; sgelman@uw.edu
[2] Department of Earth, Atmospheric, and Planetary Sciences, Massachusetts Institute of Technology, Cambridge, MA 02139, USA; ltelkins@mit.edu, seager@mit.edu
[3] Department of Physics, Massachusetts Institute of Technology, Cambridge, MA 02139, USA
Received 2011 January 7; accepted 2011 April 18; published 2011 June 17

ABSTRACT

We model the geodynamical evolution of super-Earth exoplanets in synchronous rotation about their star. While neglecting the effects of a potential atmosphere, we explore the parameter spaces of both the Rayleigh number and intensity of incoming stellar flux, and identify two main stages of mantle convection evolution. The first is a transient stage in which a lithospheric temperature and thickness dichotomy emerges between the substellar and the antistellar hemispheres, while the style of mantle convection is dictated by the Rayleigh number. The second stage is the development of degree-1 mantle convection. Depending on mantle properties, the timescale of onset of this second stage of mantle evolution varies from order 1 to 100 billion years of simulated planetary evolution. Planets with higher Rayleigh numbers (due to, for instance, larger planetary radii than the Earth) and planets whose incoming stellar flux is high (likely for most detectable exoplanets) will develop degree-1 mantle convection most quickly, on the order of 1 billion years, which is within the age of many planetary systems. Surface temperatures range from 220 K to 830 K, implying the possibility of liquid water in some regions near the surface. These results are discussed in the context of stable molten magma ponds on hotter planets, and the habitability of super-Earths which may lie outside the Habitable Zone.

Key words: convection – methods: numerical – planetary systems – planets and satellites: general – stars: individual (CoRoT-7, Gliese 581)

1. INTRODUCTION

Throughout the last decade there has been escalating work to model the internal structure, composition, evolution, and habitability of super-Earths (e.g., Kuchner 2003; Léger et al. 2004; Ehrenreich et al. 2006; Valencia et al. 2006, 2007a, 2007b). The extremely small semimajor axes of many exoplanet orbits suggest several new processes in planetary evolution that do not appear to have occurred in our solar system. Several studies, for example, characterize the effects of tidal heating on rocky planets (Jackson et al. 2008a, 2008b, 2008c; Barnes et al. 2008) and work to constrain surface temperatures from observables such as star size, planet size, semimajor axis, eccentricity, and obliquity. Recent geodynamical studies have studied the possibility and detectability of volcanism on rocky extrasolar planets (e.g., Kite et al. 2009; Kaltenegger et al. 2010). Others have addressed problems specific to tidally locked planets, such as magnetosphere (Grieβmeier et al. 2005) and climate (Joshi 2003) dynamics. The aim of this work is to further add to this library with particular attention to the effect of a tidally locked orbit on the mantle convection structure and long-term geodynamical evolution of terrestrial exoplanets.

Synchronous rotation refers to an orbit in which one rotation of the body takes precisely the same amount of time as one revolution about the orbital center. This also means that, in the case of a planet, one day is equal to one year, and one hemisphere will always be star-facing, and the other will never be. Tidal-lock occurs when a star's rotation and mass raise tides on a planet, decaying its orbit, and despinning it.

One of the main hypotheses tested here is whether low-degree mantle convection may occur due to fixed stellar heating on a synchronously rotating planet. Spherical harmonic degree-1 convection refers to a single pair of convection cells in a spherical body, and implies the presence of a single upwelling and a single downwelling in opposite poles. Previous work has suggested and explored low-degree convection, and is briefly reviewed in the discussion.

In the following section we formulate a numerical model to test tidal-lock boundary conditions on a convecting mantle. This simple model does not treat internal frictional tidal heating or atmospheric heat transport or insulation. We analyze mantle convection patterns through deep geologic time and calculate regions of possible stable liquid water near the planetary surface. From this we discuss the possibility of extreme temperatures that would permit localized magma oceans around the substellar point. Finally, we explore implications for the habitability of tidally locked Earth-like planets.

2. NUMERICAL METHODS

Numerical models have been formulated using SSAXC, a spherical axisymmetric version of the two-dimensional finite element code ConMan (King et al. 1990). ConMan models incompressible, infinite-Prandtl number thermochemical convection by solving the equations for conservation of mass,

$$\nabla \cdot \mathbf{u} = 0, \tag{1}$$

momentum,

$$\nabla^2 \mathbf{u} = \nabla p + Ra\, T\, \hat{\mathbf{z}}, \tag{2}$$

and energy,

$$\frac{\partial T}{\partial t} = -\mathbf{u} \cdot \nabla T + \nabla^2 T, \tag{3}$$

where $\mathbf{u}$ is the dimensionless velocity, T is the dimensionless temperature, p is the dimensionless pressure, $\hat{\mathbf{z}}$ is the unit vector in the vertical direction, and t is the dimensionless time.

The Prandtl is the ratio of momentum diffusivity to thermal diffusivity: $\mathrm{Pr} = \frac{\nu}{\alpha}$, where ν is kinematic viscosity and α is thermal diffusivity. In mantle silicates, viscosity is much greater than thermal diffusivity, and so SSAXC is appropriate for this application. All material properties used in these convection calculations are combined into the thermal Rayleigh number, *Ra*, which indicates the presence and vigor of convection, given by

$$Ra = \frac{\rho g \alpha \Delta T d^3}{\kappa \eta_0}, \quad (4)$$

where g is the acceleration due to gravity, α is the coefficient of thermal expansion, ΔT is the temperature drop across the mantle, d is the depth of the mantle, κ is the thermal diffusivity, and η_0 is the reference viscosity. The reference viscosity is the dimensional value of the viscosity low when the mantle is at the reference temperature. At temperatures below the reference temperature, the mantle viscosity rises, while at higher temperatures, viscosity falls. The reference viscosity is therefore a rough, average viscosity for the convecting mantle, neglecting pressure or viscosity law dependencies. Here we use a value of 10^{22} Pa s, which is reasonable for the Earth's mantle (neglecting the asthenosphere and hydrous material in subduction zones, which would have a few orders of magnitude lower viscosity than the rest of the mantle; Turcotte & Schubert 2002). SSAXC calculates a temperature-dependent viscosity based on the Arrhenius equation:

$$\eta(T) = \eta_0 e^{E^* \left(\frac{1+T_0}{T-T_0} - 1 \right)}, \quad (5)$$

where E^* is activation energy and T_0 is the temperature offset, set to 273 K.

Numerical experiments were benchmarked against Earth before being used to model exoplanetary systems. Intense stellar flux and attendant steep temperature gradients near the planetary surface requires high resolution grids, consisting here of 300 tangential nodes by 150 radial nodes. In most models presented here, initial internal mantle temperatures were set to a potential temperature of 1300 K. We assumed an initial lithosphere over the top 5% of the planetary radius, where lithosphere is defined simply by the region where heat is transferred conductively due to high viscosity produced by low surface temperatures. Our initial temperature conditions for this lithosphere consisted of a uniform temperature gradient between the mantle temperature at depth and 273 K at the surface. The evolutionary pathways of super-Earths prior to tidal-lock are not known, and this forms a simple and plausible initial condition. Two additional experiments were conducted with an initial internal mantle potential temperature at 1700 K, which explores the sensitivity of our results on initial internal thermal conditions. No significant difference was observed in the resulting planetary evolution between these two initial mantle potential temperature assumptions.

The stellar flux arriving at the planet is strongest at the substellar point ($\theta = 0$) and decays to zero at the terminator ($\theta = \frac{\pi}{2}$); the far-side ($\frac{\pi}{2} < \theta < \pi$) will receive no stellar flux. Every surface element radiates as a blackbody at each time step. Radiative fluxes are based on the Stefan–Boltzmann equation: $F = \sigma T^4$, where F is the radiative energy flux, σ is the Stefan–Boltzmann constant, and T is the temperature of the radiative body or element. From this flux we calculate the temperature of the surface of the solid silicate planet using $\Delta F = m C_p \Delta T$, where m is the mass (or density times volume: $\rho\, dx^2\, dz$), C_p is the specific heat capacity, and ΔT is the change in temperature; finally, dx and dz are the length and depth (respectively) of the surface elements in the numerical model grid.

Table 1
SSAXC Mantle Convection Parameters

Symbol	Parameter	Value
C_p	Specific heat capacity	1250 J (kg · K)$^{-1}$
F	Stellar flux	550 W m^{-2}
		1300 W m^{-2}
		5400 W m^{-2}
Ra	Thermal Rayleigh number	3×10^6
		3×10^7
		2×10^8
		1×10^9
T_{scale}	Mantle potential temperature	1300 K
		1700 K
α	Coefficient of thermal expansion	3×10^{-5} K^{-1}
η_0	Reference viscosity	10^{22} Pa · s
κ	Thermal diffusivity	10^{-6} m^2 s^{-1}
ρ	Density	3300 kg m^{-3}

For the stellar temperature addition, T_{in}, on the star-side of the planet at each time step, this flux must be multiplied by a term describing the ratio of energy radiated at the surface of the star and that at the planet's distance: $\frac{4\pi R_*^2}{4\pi a^2}$, where R_* is the star's radius and a is the planet's semimajor axis. This gives

$$T_{\mathrm{in}} = \frac{R_*^2\, \sigma\, T_*^4\, dt}{a^2\, \rho\, dx^2\, dz\, C_p}, \quad (6)$$

where T_* is the star's effective temperature, dt is the Courant time step, ρ is the density of rock in the planet, and dx and dz reference the width and depth of an element, respectively. An analogous derivation for the planet's radiative flux out yields

$$T_{\mathrm{out}} = \frac{\sigma\, T_p^4\, dt}{\rho\, dx^2\, dz\, C_p}, \quad (7)$$

where T_p is the temperature of each element at the beginning of the calculation of that time step. Equations (6) and (7) are added and subtracted (respectively) to each temperature calculation for the surface elements on the star-side; only Equation (7) is subtracted from the temperature calculations for the far-side surface elements.

Since this study is focused in understanding the isolated long-term effects of stellar flux and blackbody radiation during synchronous rotation on Earth-like planets, we make several simplifying assumptions. First, internal compositional variations are assumed to be negligible, and therefore a uniform approximate dry peridotite mantle is used. No interior phase changes were included in the mantle. Material input parameters and other constants throughout these numerical experiments are listed in Table 1.

We also do not include atmospheres in these simulations. Any atmospheres on these relatively small planets may be removed by high surface temperatures and stellar bombardment. The presence of an atmosphere on a super-Earth has not yet been observed, though several theoretical approaches for atmosphere detection have been proposed (e.g., Miller-Ricci et al. 2009; Seager & Deming 2009). Importantly, for cooler planets, particularly those orbiting M-stars, the atmosphere-less assumption may be poor, albeit necessary in our models.

Table 2
Sample of Known Super-Earths

Name	$m \sin i$ ($M_\oplus$)	Semimajor Axis (AU)	Stellar Flux (W m^{-2})
Gliese 581 d[1]	7.09	0.22	550
Gliese 581 g[12]	3.1	0.146	1200
Gliese 581 c[1]	5.36	0.07	5400
HD 285968 b[2]	8.42	0.066	12,100
HD 40307 d[3]	9.15	0.134	21,500
GJ 1214 b[4]	5.69	0.014	23,300
Gliese 581 e[1]	1.94	0.03	28,800
Gliese 876 d[5]	6.36	0.021	45,400
HD 40307 c[3]	6.87	0.081	58,700
HD 156668 b[11]	4.15	0.05	140,000
HD 7924 b[6]	9.22	0.057	165,000
HD 40307 b[3]	4.20	0.047	175,000
CoRoT 7 c[7]	8.39	0.046	339,000
61 Vir b[8]	5.09	0.05	405,000
HD 1461 b[9]	7.60	0.063	409,000
55 Cnc e[10]	7.63	0.038	848,000
CoRoT 7 b[7]	4.80	0.0172	2,430,000

References. (1) Mayor et al. 2009a; (2) Forveille et al. 2009; (3) Mayor et al. 2009b; (4) Charbonneau et al. 2009; (5) Correia et al. 2010; (6) Howard et al. 2009; (7) Queloz et al. 2009; (8) Vogt et al. 2010a; (9) Rivera et al. 2010; (10) Fischer et al. 2008; (11) Howard et al. 2011; (12) Vogt et al. 2010b.

However, our results can be extrapolated to hotter super-Earths, for which this assumption may be justified. Future work should consider the validity of this assumption, since a significant atmospheric presence would redistribute heat and dampen the effect of a strong, fixed stellar heating.

Finally, previous work has shown that the effect of orbital tides on a planet without a perfectly circular orbit may be a potentially large source for internal heating (Jackson et al. 2008a, 2008b, 2008c; Barnes et al. 2008). Here we assume negligible deviations in both obliquity and eccentricity. Future work should compare the effect of tidal heating with fixed stellar heating to determine the total effect on planets with noncircular orbits at various semimajor axes around massive stars.

3. RESULTS

Our numerical experiments explore the parameter spaces of both Rayleigh number and stellar flux. A starting *Ra* was calculated for an Earth-like planet using parameters defined in Table 1. Variations in *Ra* spanned three orders of magnitude, from 3×10^6 to 1×10^9; this wide range can be produced by changes in several parameters, including mantle viscosity, interior planetary temperature, and planetary radius. Here we assume a temperature-dependent mantle viscosity with a reference value of 10^{22} Pa s, and an approximately adiabatic mantle at either 1300 K or 1700 K, which allows us to use variations in *Ra* as a way to investigate varying planetary radius. Stellar flux variations spanned 550–5400 Wm^{-2}. Note that Earth, and the newly discovered Gliese 581 g, correspond to approximately 1300 W m^{-2}, and from Table 2, Gliese 581 d and c to 550 and 5400 W m^{-2}, respectively. A summary of experimental conditions and results can be found in Table 3.

In all experiments the large-scale degree-1 mantle convective structure developed, and we will generally use the timescale associated with development of this structure for comparison and evaluation of our results. However, in some cases, this timescale far exceeded the age of the universe, and hence not all planets in tidal-lock may have developed degree-1 convection yet. For a planet to develop degree-1 convection in under approximately 5 billion years, both the stellar flux the planet receives and the *Ra* must be at the high end of the ranges explored in this study. This result is examined conceptually in Section 4.1.

Table 3
Summary of Experimental Results

Ra	Stellar Flux (W m^{-2})	Mantle Temp. (K)	Timescale (10^9 yr)
3×10^6	550	1300	10^2
3×10^6	1300	1300	10^2
3×10^6	5400	1300	10^1
3×10^7	5400	1300	10^1
2×10^8	5400	1300	10^1
2×10^8	5400	1700	10^1
1×10^9	5400	1300	10^0
1×10^9	5400	1700	10^0

In all simulations, we have identified two main evolutionary stages in mantle convection. The first comprises a period of high-degree convection dictated by the *Ra*. During this stage, upwellings and downwellings are pervasive, while the substellar surface radiatively warms and the antistellar surface radiatively cools while slowly growing thicker. In high *Ra* regimes, narrow upwellings and downwellings occur throughout the mantle with no clear periodic spacing. At 10 evenly spaced time step panels throughout this stage in the $Ra = 1 \times 10^9$ simulation, we counted downwellings and characterized them as "star-side" or "dark-side." We find that generally more lithospheric drips occurred on the star-side of the planet than on the dark-side (95 to 77 drips, respectively). Some of these convective cells span the entire depth of the mantle, while others are confined largely to the upper third of the mantle. There did not appear to be any correlation of the depth or width of a lithospheric drip with the hemispheric surface dichotomy. In the low *Ra* end member ($Ra = 3 \times 10^6$), as expected, thick, periodic, alternating upwellings and downwellings form.

The second stage of evolution is the formation of degree-1 mantle convection. Figure 1 shows the time evolution of an Earth-like planet receiving a flux corresponding to Gliese 581 c (5400 W m^{-2}). Figure 2 is the time evolution of a planet with three orders of magnitude higher *Ra*, but again receiving the same stellar flux as Gliese 581 c. Comparison between these figures shows the important control *Ra* has on development of degree-1 convection and overall mantle cooling patterns. Since both material properties and mantle geometry are collapsed in the *Ra*, any combination of parameters which raise this value (such as larger mantle depth, a greater temperature gradient, or lower mantle viscosity) will promote a faster development of degree-1 convection. Based on these results, while stellar flux influences the long-term structure of mantle convection with a hot substellar region and a cool antistellar region, the *Ra* plays a primary role in determining the timescale of onset of this structure.

Figure 3 shows near-surface temperatures (one node from the surface boundary) for both Earth-like planets ($Ra = 3 \times 10^6$) receiving a range of stellar fluxes (colored curves), and planets with larger *Ra* (black curves). In the case of an Earth-like set of mantle parameters ($Ra = 3 \times 10^6$), generally, near-surface temperatures remain constant throughout the evolution of the planet. While lithospheric thicknesses change, and hence the geothermal gradient changes, due to the overwhelming

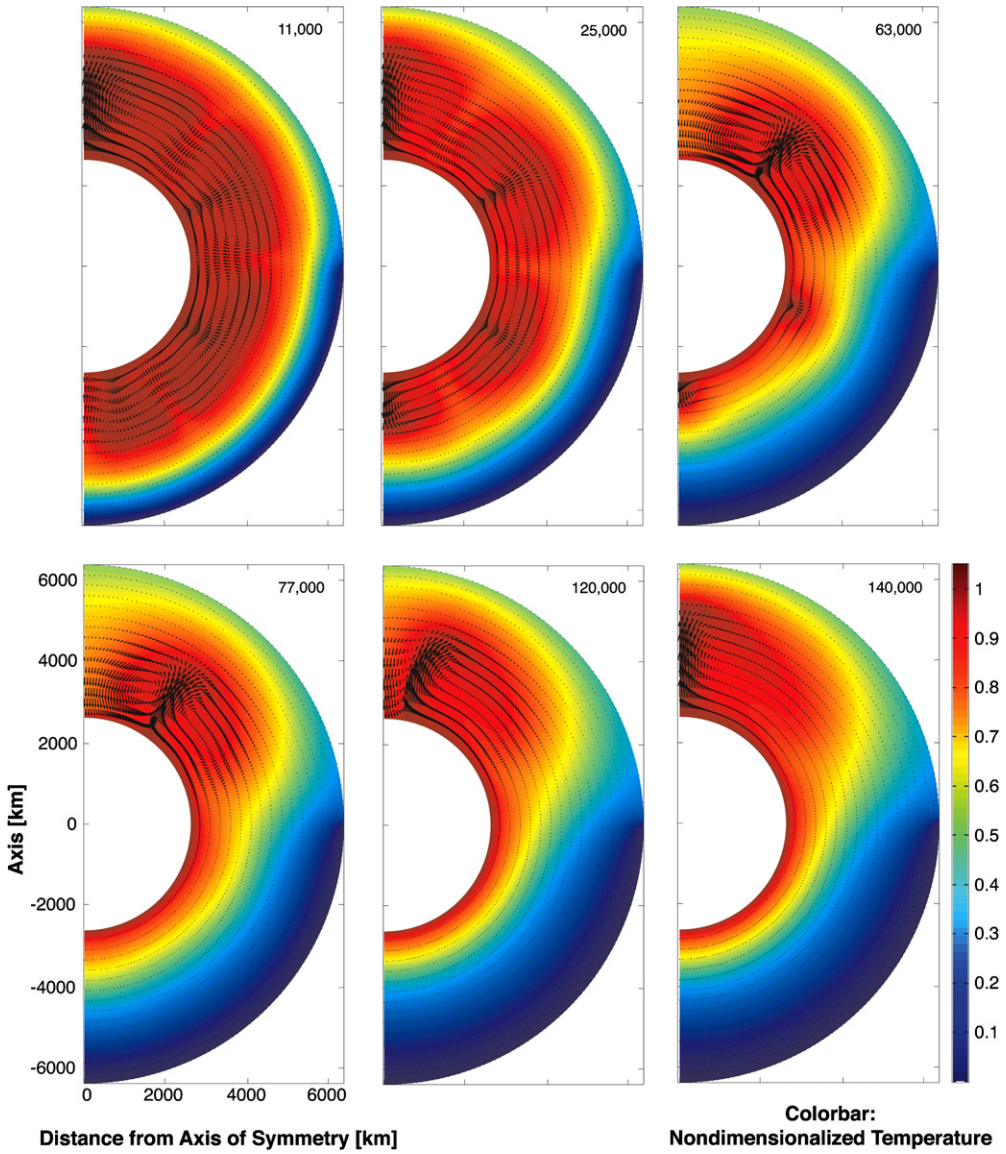

Figure 1. Modeled time evolution of a tidally locked terrestrial exoplanet whose stellar flux corresponds with that of Gliese 581 c ($F = 5400$ W m^{-2}), and whose mantle properties and geometry are similar to Earth's ($Ra = 3 \times 10^6$; see Table 1 and the text for details). Simulated time in millions of years since model initiation is given at the top of each panel. Stellar flux arrives from the top of the page. Color corresponds to nondimensionalized temperature. Initial mantle temperature, as well as the factor of temperature dimensionalization, is set to 1300 K. Arrows indicate direction and magnitude of local convective velocity.

control of both stellar heating and radiative heat loss to space, surface temperatures can remain largely stable, even with a striking dichotomy between substellar to antistellar regions. Substellar temperatures range from approximately 600 K in the Gliese 581 d case (flux is 550 W m^{-2}) to 830 K in the Gliese 581 c case (flux is 5400 W m^{-2}). Temperatures at the terminator vary far less, from 310 to 350 K, and temperatures at the substellar point are independent of stellar flux. Figure 3 also highlights the range of temperatures which permit stable liquid water at one bar pressure. For all cases at the low *Ra* end member, temperatures from the substellar point to intermediate star-side regions fall within this tentative range allowing the possibility of stable liquid water at or near the surface. It should be repeated, however, that the presence of an atmosphere, not modeled here, would more evenly distribute heat across the surface of the planet and, depending on the potential atmospheric composition, may also insulate and warm the planet. Our geophysical results would therefore be most applicable for hotter planets whose atmospheres may not be sustainable due to stellar bombardment.

The surface temperatures of the high *Ra* end member receiving a flux equivalent to Gliese 581 c (5400 W m^{-2}) are plotted in black in Figure 3. Substellar temperatures are approximately 100 K cooler than in the lower *Ra* case, and have a significant temporary plateau corresponding to the initiation of degree-1 convection. Temperatures at the terminator are constant, but approximately 100 K warmer than the lower *Ra* case, while antistellar temperatures, on the other hand, are somewhat cooler. Similar to the low *Ra* cases, there is a region which would tentatively allow for stable liquid water near the surface in the intermediate regions of the "dark" side of the planet.

4. DISCUSSION

4.1. Degree-1 Mantle Convection

Mantle convection on Earth is driven primarily by heat loss from our planet's interior. This heat comes mainly from the decay of radiogenic elements (∼75%) and secular cooling through planetary evolution (∼25%), as well as conductive

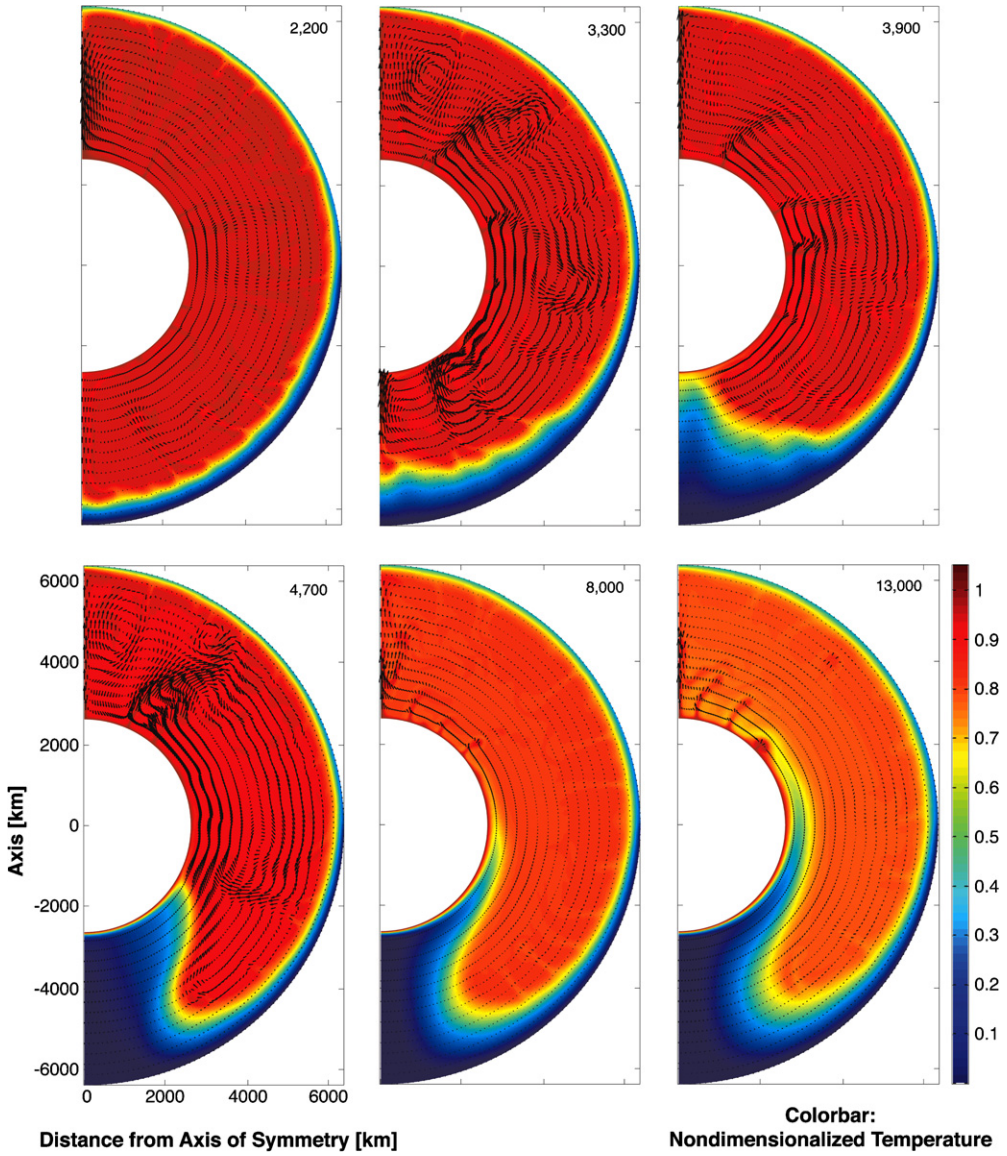

Figure 2. Modeled time evolution of a tidally locked terrestrial exoplanet whose stellar flux corresponds with that of Gliese 581 c ($F = 5400$ W m^{-2}), but whose *Ra* is approximately three orders of magnitude greater than that of Earth's ($Ra = 1 \times 10^9$). This increase in *Ra* may be due to variations in a range of parameters (see Equation (4)), but two possibilities are lower mantle viscosity, or approximately five times larger planetary radius (though such a large radius may imply retention of light volatiles such as H and He, which would imply a gaseous planet rather than terrestrial). Simulated time in millions of years since model initiation is given in the top of each panel. Note that if the increase in *Ra* is a result of a higher planetary radius, scaling relationships imply a factor of nearly 25 increase in simulated time. Stellar flux arrives from the top of page. Color corresponds to nondimensionalized temperature. Initial mantle temperature, as well as the factor of temperature dimensionalization, is set to 1300 K. Arrows indicate direction and magnitude of local convective velocity.

transfer from the core to the mantle; heat is then lost through the conductive lithosphere and radiated to space (Turcotte & Schubert 2002). Therefore, between the core and the lithosphere, there is a temperature gradient; cool material near the lithosphere then sinks due to thermal contraction and densification while warm material rises due to thermal expansion. Although whether the Earth maintains a single or multi-layer convective structure is still unresolved (e.g., see Tackley 2000), these convection currents populate the mantle relatively evenly with upwellings and downwellings. However, our results show that for tidally locked planets, thermal control of mantle convection passes from the planetary interior (the temperature gradient between the lithosphere and the core) to the exterior (the gradient along the surface of the lithosphere). The hot substellar point produces a stable region of upwelling, permanently changing the mantle convective pattern.

These results therefore demonstrate that surface temperature can force patterns of mantle convection in terrestrial planets, as first suggested by Pekeris (1935). In previous work, several parameters, besides *Ra* and surface boundary conditions, have been shown to be potentially significant controls on the development of low-degree convection. These parameters include internal heating, phase changes, depth-dependent viscosity, and a particularly weak asthenospheric layer (e.g., Ratcliff et al. 1997; Zhong & Zuber 2001; McNamara & Zhong 2005; Roberts & Zhong 2006). Here we add stellar flux forcing in tidally locked planets to this list.

While planetary surface temperatures can control mantle convective patterns, the effect of varying *Ra* largely dictates the timescale of development of low-degree convection. At the limit of low *Ra* heat diffusion dominates, while at high *Ra* advection dominates. It follows that at lower *Ra* (but still significantly

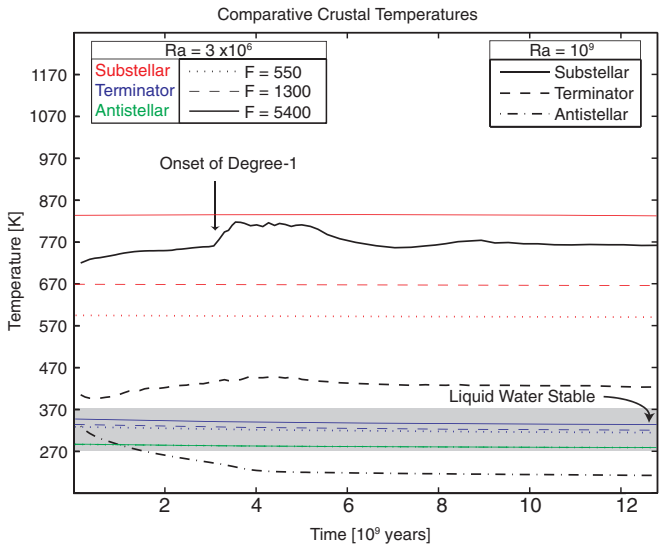

Figure 3. Summary of temperature results at approximately 20 km depth (one node below the surface boundary) for a variety of incoming stellar fluxes and mantle properties. Legend in top left corresponds to models using a $Ra = 10^6$ (Earth-like); line style (solid, dashed, dotted) corresponds to stellar flux while color corresponds to location on planet (substellar, terminator, antistellar). Legend on top right corresponds to a model using a $Ra = 10^9$; flux is set to 5400 W m^{-2}; line style now corresponds to location on planet (substellar, terminator, antistellar) and color is black. Gray shaded region indicates temperatures at which liquid water would be stable at pressures of one bar.

higher than the critical Rayleigh number for convection), the characteristic timescale of convection is longer than at high *Ra*. We found that three orders of magnitude difference in *Ra*, which can correspond to a factor of five in planetary radius if other mantle material properties remain constant, corresponded to two orders of magnitude difference in the timescale to onset of degree-1 convection. Moreover, the difference in *Ra* also had implications for the morphology of the degree-1 convective pattern. At the low *Ra* extreme, the antistellar hemisphere cooled fairly uniformly resembling simple conductive heat transfer, while at the higher *Ra* end member, the antistellar point develops a more prominent downwelling with corner flow (compare Figures 1 and 2). This type of circulation must be included when considering the possibility and character of plate tectonics on tidally locked super-Earths.

Our initial conditions for these models were radially uniform, and therefore apparently antithetical to the stable degree-1 pattern resulting from this strong substellar point heating. Likewise many planets will not begin in tidal-lock, but eventually despin if given enough time. Once planets are in tidal-lock, their mantles will likely need additional evolutionary time to transition to degree-1 convection. Based on our results, we expect any planets which have become tidally locked to develop these patterns in timescales determined primarily by *Ra* and stellar flux. The transition from radially uniform mantle convection to degree-1 convection would likely be accompanied by increased volcanism near the substellar point, and suppressed volcanism on the antistellar side. This is because upwelling mantle may be expected to experience decompression melting similar to that in mid-ocean ridges or ocean islands on Earth, while downwelling mantle would be unlikely to experience any melting. In addition, crustal temperatures generally become elevated on the substellar hemisphere of the planet, potentially allowing increased magma production, while the opposite would be true for the antistellar hemisphere.

The longevity of this pattern of convection is determined by the efficiency of planetary heat loss. Planets begin with hot interiors, due to the energy released through accretion and radioactive decay. If a star also begins more faint ("faint young sun"; Sagan & Mullen 1972), the combined effect is an increasing amplitude of the surface temperature dichotomy through the life of a planet. Eventually, the only source of planetary heating would be from its star. Hence, once the degree-1 convective structure is in place, it may remain stable until the planet cools enough to stop mantle convection entirely.

With a stable annulus of clement conditions near the surface of these tidally locked planets, a potential habitable oasis might exist, even in planets which lie beyond the traditional habitable zone. While an atmosphere seems like a precondition for potentially detecting life on an exoplanet, realistically, subsurface conditions may be habitable over long timescales even on planets without an appreciable atmosphere. This seems especially plausible if some sort of an aquifer, or permeable liquid-saturated layer, can exist to allow for efficient nutrient transfer.

4.2. Surficial Magma Ponds

While in the models presented here temperatures do not rise above approximately 850 K, several detected exoplanets receive higher stellar fluxes than we are able to model (Table 2) and would be tentatively expected to have significantly higher substellar temperatures. Depending on mineralogy and volatile content of the upper mantle and lithosphere, near-solidus partial melting may begin at temperatures as low as 870°C for felsic compositions, or 1370 K for mafic compositions. If substellar temperatures are high enough, and stable for long periods of time, they may partially melt the surface in the hottest regions of the planet, producing stable, long-term "magma ponds," or localized magma oceans.

Localized magma oceans have been studied previously in order to understand the effects of large impactors early in terrestrial planet evolution (e.g., Tonks & Melosh 1993; Reese & Solomatov 2006; Watters et al. 2009). A significant difference between the dynamics of impact-induced transient molten regions and stellar flux-induced magma ponds is long-term evolution and stability. In the former, crystallization timescales depend on the depth, extent, composition, and, in general, the cooling efficiency of the region, while in the latter, the same is true but, given enough stellar heating, large-scale magma ponds may persist indefinitely. While estimating the dimensions and dynamics of such a pond is complex (for example, considering various compositions and their solidi, extent of melting, melt extraction efficiency, isostatic rebound of the solid floor, and internal convection), if the arriving stellar flux delivers more energy than is lost by the convecting magma pond, we can assume that the feature will be stable over long timescales.

According to Kraichnan (1962), the heat lost from the top of a cooling magma pond, F_m, in a high Prandtl number convective regime is

$$F_m \sim 0.089 Ra^{1/3}. \quad (8)$$

After Reese & Solomatov (2006), we combine Equations (4) and (8) and redimensionalize to obtain

$$F_m = 0.089 k (T_p - T_s)^{4/3} \left(\frac{\rho_l \alpha g}{\eta_l \kappa} \right)^{1/3}, \quad (9)$$

where k is thermal conductivity, ρ_l is the silicate liquid density, α is the coefficient of thermal expansion, η_l is the silicate liquid

Table 4
Magma Pond Calculation Parameters

Symbol	Parameter	Value
k	Thermal conductivity	$4\text{W}\,(\text{m}\cdot\text{K})^{-1}$
ρ_l	Silicate liquid density	$3300\ \text{kg m}^{-3}$
α	Coefficient of thermal expansion	$2\times10^{-5}\ \text{K}^{-1}$
η_l	Silicate liquid dynamic viscosity	$10^{-1.2}\ \text{Pa}\cdot\text{s}$
κ	Thermal diffusivity	$1\times10^{-6}\ \text{m}^2\ \text{s}^{-1}$
T_p	Potential temperature	1670 K
T_s	Surface temperature	1470 K

Note. T_p and η_l for magma with peridotite composition obtained from Bottinga & Weill (1972 and references therein).

dynamic viscosity, κ is the thermal diffusivity, T_p is the potential temperature, and T_s is the surface temperature. To obtain values for these simple calculations, we assume a sufficiently high surface temperature, $T_s \approx 1470$ K, such that peridotite would be molten. We assume that the liquid magma pond will have a thin surface boundary layer, with a change in viscosity by a factor of 10 between the boundary layer and the lower convecting material (e.g., Zaranek & Parmentier 2004). A mafic silicate melt at 1470 K at the surface corresponds to a viscosity of $\sim10^{-0.2}$; once we decrease this by an order of magnitude, we expect the viscosity of the convecting fluid to be $\sim10^{-1.2}$, which correlates to a potential temperature, T_p, of ~1670 K (Bottinga & Weill 1972, Figure 7, and references therein). A summary of the parameters and values used in these calculations is given in Table 4.

To a first order, if the flux released by the partially molten surface remains less than or equal to the flux received from the star, $F_s = \sigma T_*^4$, then the magma ocean should be stable over long timescales. Though still neglecting the presence of an insulating atmosphere, a simple calculation of maximum semimajor axes for the stability of an exposed molten surface around various stars which have detected super-Earths is shown in Figure 4. For our solar system, in order for a localized magma ocean to be stable on an Earth-like planet, the semimajor axis must be less than ~0.12 AU. The known planets which, based on this calculation, are able to sustain a magma ocean for long timescales from fixed stellar heating are CoRoT 7 b, CoRoT-7 c, HD 7924 b, 55 Cnc e, 61 Vir b, HD 1461 b, and HD 40307 b. Though several other exoplanets actually have significantly smaller semimajor axes than the above, they orbit significantly weaker stars (for example, Gliese 581 e is around an M-star) which do not deliver enough stellar flux, even for close-in planets, to match the efficiency of heat loss from a magma ocean.

A planet with a large localized magma ocean will become asymmetric based on the differences in density between molten and solid silicates. Analogous to glacial rebound on Earth, the solid mantle underlying the magma pond will isostatically rebound under the lighter load, causing magma to spill out of the pond and spread beyond the region of stellar heat sufficient to melt silicates. The overflowing magma will crystallize, forming lava levées around the magma pond. At the same time, the magma pond will be melting back into the planetary interior to its original depth, determined by stellar flux.

During melting the magma will lose its more volatile components, beginning with water, carbon, and oxygen and sulfur species, and at higher temperatures continuing to sodium, fluorine, chlorine, silicon, and potassium, possibly even to iron (for more details, see Schaefer & Fegley 2009). These species,

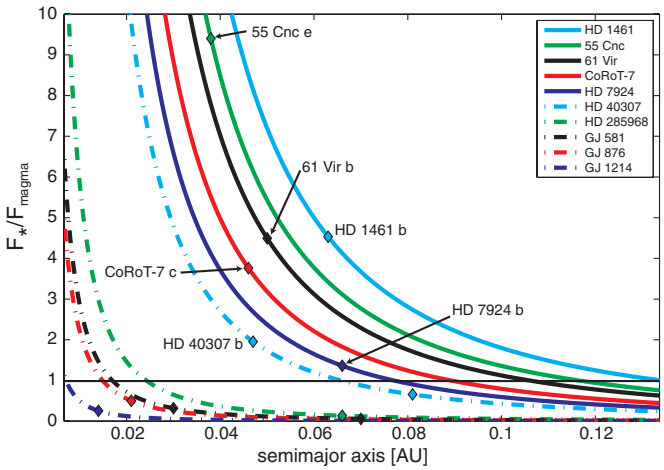

Figure 4. Flux ratio of incoming stellar radiation over released heat from a magma pond is plotted against semimajor axis. If the amount of incoming heat is greater than the heat released by a convecting surficial magma pond (i.e., a planet is plotted above the straight black line at $\frac{F_*}{F_{\text{magma}}} = 1$), then the magma pond may be stable over geologically long timescales. Several super-Earth-bearing star systems are plotted, and we find the following planets (in the absence of an atmosphere) could harbor a stable magma pond at their substellar points: CoRoT-7 b, CoRoT-7 c, HD 40307 b, 55 Cnc e, 61 Vir b, HD 1461 b, and HD 7924 b.

released into a transient or permanent atmosphere, leave behind an increasingly refractory liquid and solid silicate planet. The magma pond will therefore require increasing stellar flux to produce the same depth of melt. If the volatile components cannot be recycled back into the planetary interior through a process like plate tectonics, then the magma pond will eventually solidify as the planetary interior composition's melting temperature rises above the input from the star. Any degassing of nonrecycled species may be detectable indications of this process. An additional source of mantle degassing may be volcanism, which we would qualitatively expect to be focused near the substellar point. However, the presence or extent of any plate tectonic activity could greatly influence the effect of this potential devolatilization source.

5. CONCLUSIONS AND IMPLICATIONS FOR HABITABILITY

We have explored the effect of synchronous rotation on terrestrial exoplanetary mantle and surface evolution. While planets around M-stars such as Gliese 581 may be expected to have atmospheres in general (which were not modeled here), our results provide a baseline geodynamical framework upon which such complexities may be added. Exploring a range of orbital conditions, from fluxes corresponding to Gliese 581 d to Gliese 581 c, we found two main phases of planetary evolution: a transient stage of pervasive high-degree convection and a culminating period of degree-1 convection. The timescale dictating the transition between these two evolutionary stages is controlled largely by the Rayleigh number. We find a gradient of surface temperatures ranging from 850 K to below 270 K, and hence regions either at the surface, or shallow subsurface, which may support stable liquid water. Lastly, we extrapolate our results to planets receiving higher stellar fluxes. With sufficiently high temperatures, a silicate lithosphere may melt and even support persisting localized magma oceans.

Two aspects of planetary evolution explored here may be directly detectible. A large temperature dichotomy on an

atmosphere-less tidally locked planet may be detectible by measuring a thermal phase curve as described by Seager & Deming (2009). Second, with advances in detection techniques, potentially degassing magma ponds may provide a transient or permanent atmosphere which can be detected in the future, as has been done for transiting giant gas planets (e.g., Charbonneau et al. 2002; Vidal-Madjar et al. 2010).

The search for exoplanets has produced an array of exotic planets whose orbital conditions and surface environments are not found anywhere in our solar system. At the core of the exoplanet search is the hunt for habitable environments beyond Earth. Many workers propose that liquid water is a pre-condition for life due to its efficient transport of biochemical material and link to carbon-based biology (e.g., Hart 1978; Kasting & Catling 2003). This has led many to define a habitable zone: a range of semimajor axes in which stellar heating allows an Earth-like planet to have surface temperatures permitting liquid water. Using this definition, weak stars such as Gliese 581 may support tidally locked planets just outside the habitable zone which would normally be dismissed as uninhabitable. However, based on these results, a planet which does not strictly lie within the habitable zone may still support liquid water on its surface, or shallow subsurface, in certain regions of the planet. Thus, instead of assuming or precluding liquid water on planets like Gliese 581 c and d, tidally locked mantle and climate patterns (Joshi 2003) must be combined and assessed to determine the surface environment, keeping in mind this may vary greatly from the substellar to antistellar regions.

We gratefully acknowledge funding from NSF Astronomy CAREER grant 0747154, the MIT Undergraduate Opportunities Program, and from NSF REU. We also acknowledge preliminary work done by Anita Ganesan. This manuscript benefited from the thoughtful review of an anonymous reviewer. Lastly, we thank Steven Kawaler for his editorial efforts.

REFERENCES

Barnes, R., Raymond, S. N., Jackson, B., & Greenberg, R. 2008, Astrobiology, 8, 557
Bottinga, Y., & Weill, D. F. 1972, Am. J. Sci., 272, 438
Charbonneau, D., Brown, T. M., Noyes, R. W., & Gilliland, R. L. 2002, ApJ, 568, 377
Charbonneau, D., et al. 2009, Nature, 462, 891
Correia, A. C. M., et al. 2010, A&A, 511, A21
Ehrenreich, D., des Etangs, A. L., Beaulieu, J.-P., & Grasset, O. 2006, ApJ, 651, 535
Fischer, D. A., et al. 2008, ApJ, 675, 790
Forveille, T., et al. 2009, A&A, 493, 645
Grießmeier, J.-M., Stadelmann, A., Motschmann, U., Belisheva, N. K., Lammer, H., & Biernat, H. K. 2005, Astrobiology, 5, 587
Hart, M. H. 1978, Icarus, 33, 23
Howard, A. W., et al. 2009, ApJ, 696, 75
Howard, A. W., et al. 2011, ApJ, 726, 73
Jackson, B., Greenberg, R., & Barnes, R. 2008a, ApJ, 681, 1631
Jackson, B., Greenberg, R., & Barnes, R. 2008b, ApJ, 678, 1396
Jackson, B., Barnes, R., & Greenberg, R. 2008c, MNRAS, 391, 237
Joshi, M. 2003, Astrobiology, 3, 415
Kaltenegger, L., Henning, W. G., & Sasselov, D. D. 2010, AJ, 140, 1370
Kasting, J. F., & Catling, D. 2003, ARA&A , 41, 429
King, S. D., Raefsky, A., & Hager, B. H. 1990, Phys. Earth Planet. Inter., 59, 195
Kite, E. S., Manga, M., & Gaidos, E. 2009, ApJ, 700, 1732
Kraichnan, R. H. 1962, Phys. Fluids, 5, 1374
Kuchner, M. J. 2003, ApJ, 596, L105
Léger, A., et al. 2004, Icarus, 169, 499
Mayor, M., et al. 2009a, A&A, 507, 487
Mayor, M., et al. 2009b, A&A, 493, 639
McNamara, A. K., & Zhong, S. 2005, J. Geophys. Res. Lett., 32, L01301
Miller-Ricci, E., Seager, S., & Sasselov, D. 2009, ApJ, 690, 1056
Pekeris, C. L. 1935, Geophys. J. Int., 3, 343
Queloz, D., et al. 2009, A&A, 506, 303
Ratcliff, J. T., Tackley, P. J., Schubert, G., & Zebib, Z. 1997, Phys. Earth Planet. Inter., 102, 201
Reese, C. C., & Solomatov, V. S. 2006, Icarus, 184, 102
Rivera, E. J., Butler, R. P., Vogt, S. S., Laughlin, G., Henry, G. W., & Meschiari, S. 2010, ApJ, 708, 1492
Roberts, J. H., & Zhong, S. 2006, J. Geophys. Res., 111, E06013
Sagan, C., & Mullen, G. 1972, Science, 177, 52
Schaefer, L., & Fegley, B. 2009, ApJ, 703, L113
Seager, S., & Deming, D. 2009, ApJ, 703, 1884
Tackley, P. J. 2000, Science, 288, 2002
Tonks, W. B., & Melosh, H. J. 1993, J. Geophys. Res., 98, 5319
Turcotte, D. L., & Schubert, G. 2002, Geodynamics (2nd ed.; Cambridge: Cambridge Univ. Press)
Valencia, D., O'Connell, R. J., & Sasselov, D. 2006, Icarus, 181, 545
Valencia, D., Sasselov, D., & O'Connell, R. J. 2007a, ApJ, 656, 545
Valencia, D., Sasselov, D., & O'Connell, R. J. 2007b, ApJ, 665, 1413
Vidal-Madjar, A., et al. 2010, A&A, 523, A57
Vogt, S. S., Butler, R. P., Rivera, E. J., Haghighipour, N., Henry, G. W., & Williamson, M. H. 2010b, ApJ, 723, 954
Vogt, S. S., et al. 2010a, ApJ, 708, 1366
Watters, W. A., Zuber, M. T., & Hager, B. H. 2009, J. Geophys. Res., 114, E02001
Zaranek, S. E., & Parmentier, E. M. 2004, Earth Planet. Sci. Lett., 224, 371
Zhong, S., & Zuber, M. T. 2001, Earth Planet. Sci. Lett., 189, 75